



OPEN

SUBJECT AREAS:
DRUG DEVELOPMENT
BREAST CANCER
NATURAL PRODUCTS

Received
5 January 2015

Accepted
27 February 2015

Published
19 March 2015

Correspondence and
requests for materials
should be addressed to
J.-W.Z.
(tjzhangjinwen@163.
com); G.Z.
(zhanggen888@126.
com) or Y.-H.Z.
(zhangyh@mails.tjmu.
edu.cn)

Indole diketopiperazines from endophytic *Chaetomium* sp 88194 induce breast cancer cell apoptotic death

Fu-qian Wang¹, Qing-yi Tong², Hao-ran Ma¹, Hong-feng Xu¹, Song Hu¹, Wei Ma¹, Yong-bo Xue², Jun-jun Liu², Jian-ping Wang², Hong-ping Song⁴, Jin-wen Zhang³, Geng Zhang¹ & Yong-hui Zhang²

¹Department of Pharmacy, Wuhan First Hospital, Wuhan 430022, Hubei, People's Republic of China, ²Hubei Key Laboratory of Natural Medicinal Chemistry and Resource Evaluation, School of Pharmacy, Tongji Medical College, Huazhong University of Science and Technology, Wuhan 430030, People's Republic of China, ³Tongji Hospital Affiliated to Tongji Medical College, Huazhong University of Science and Technology, Wuhan 430030, People's Republic of China, ⁴Puai Hospital Affiliated to Tongji Medical College, Huazhong University of Science and Technology, Wuhan 430030, People's Republic of China.

Diketopiperazines are important secondary metabolites of the fungi with variety bioactivities. Several species belonging to genus *Chaetomium* produce compounds of this class, such as chetomin. To identify new antitumor agents, secondary metabolites of fungus *Chaetomium* sp 88194 were investigated and three new indole diketopiperazines, Chaetocochins G (1), Oidioperazines E (2) and Chetoseminudin E (3), along with two known compounds Chetoseminudins C (4) and N-acetyl- β -oxotryptamine (5), were obtained. Chaetocochins G and Chetoseminudin E were recrystallized in CHCl₃ containing a small amount of MeOH, and their structures with absolute configuration were established by spectroscopic data interpretation and single-crystal X-ray diffraction analysis. The absolute configuration of Oidioperazines E was defined by comparing of experimental and calculated electronic circular dichroism spectra. These isolates were also evaluated the anticancer activity, and Chaetocochins G displayed more potent cytotoxicity in MCF-7 cells than the common chemotherapeutic agent (5-fluorouracil) associated with G2/M cell cycle arrest. More importantly, Chaetocochins G induced cell apoptotic death via caspase-3 induction and proteolytic cleavage of poly (ADP-ribose) polymerase, concomitantly with increased Bax and decreased Bcl-2 expression. Our findings suggested that indole diketopiperazines from endophytic *Chaetomium* sp 88194 may be potential resource for developing anti-cancer reagents.

Endophytic fungi metabolites have gained increased attention as a new resource for the discovery of new therapeutic agents^{1,2}. The endophytic fungi of the genus *Chaetomium* produce many types of secondary metabolites, such as indole diketopiperazines which are widely found as mold secondary metabolites with bioactivities including antitumor, antimicrobial, antineoplastic, and cytotoxicity effects³.

Breast cancer is one of four oncology diseases that are most widespread in the world, it also one of leading causes of cancer-related deaths in female population⁴, causing death of about 350,000 women in both developed and developing countries every year⁵.

In order to find new antitumor agents, the extracts of the fermented rice substrate of the fungus *Chaetomium cochliodes* 88194 that obtained from China Forestry Culture Collection Center (cfcc 88194) was investigated, leading to the isolation of three new indole diketopiperazines (1–3) and two known compounds (4–5)^{6,7}. Our work thereby provides three new indole diketopiperazines (1, 2, and 3), and Chaetocochins G (1) display antiproliferative effect, at least partially, due to the induction of apoptosis in MCF-7 cells.

Results and Discussion

Our present research is focused on determining the structures of indole diketopiperazines (1–5) from *Chaetomium cochliodes* 88194 and investigating the antiproliferative effect of isolates against the MCF-7 human breast cancer cell line. The results showed that Chaetocochins G exhibited cytotoxicity with IC₅₀ values of 8.3 μ g/mL (48 h). Cell cycle arrest is regarded as one of effective strategies for eliminating the cancer cells^{8,9}. Besides cell cycle, apoptosis, acting as a protective mechanism that destroys potentially harmful or damaged cells before manifestation of malignancy¹⁰, is also another key strategy for eliminating cancerous cells^{11,12}. Chaetocochins G significantly inhibits proliferation in MCF-7 cell lines, with the observation of cell cycle arrest at the G2/M phase



and activated cellular apoptosis through activation of caspase-3 and proteolytic cleavage of poly (ADP-ribose) polymerase. It also could increase Bax and decrease Bcl-2 expression.

Structure elucidation. Compound **1** was isolated as colorless needle crystals. Its molecular formula, $C_{35}H_{42}N_6O_6S_4$, was established by HRESIMS (m/z 793.1934 $[M + Na]^+$, calcd. 793.1941). Its IR spectrum showed characteristic absorptions of hydroxyl group (3399 cm^{-1}), and four carbonyl groups (1605 , 1632 , 1647 and 1667 cm^{-1}).

The ^1H NMR spectrum of **1** (Table 1) exhibited signals for four S-methyl (δ_H 2.30, s; 2.24, s; 2.10, s; 2.00, s), three N-methyl (δ_H 3.20, s; 3.12, s; 2.78, s), four methylene groups (δ_H 3.18/3.88, d; 3.34/3.58, d; 3.84/4.32, d; 3.09/3.74, d), two sets of aromatic protons (δ_H 6.73/7.04, d; 7.25/6.94, t; 6.87/7.03, t; 7.27/7.57, d), and an olefinic protons (δ_H 7.01, s). Correspondingly, the ^{13}C NMR and DEPT spectra showed the presence of the S-methyl, N-methyl, aromatic and olefinic carbons, together with five sp^2 quaternary carbons (δ_C 149.8, 127.9, 134.8, 129.6, 107.6), five sp^3 quaternary carbons (δ_C 68.6, 71.3, 72.9, 73.2, 73.4), one methines bearing heteroatoms (δ_C 81.7), and four carbonyl groups (δ_C 164.2, 165.9, 166.0, 166.6). In light of the above data, compound **1** was determined to be a chetomin-type indole diketopiperazine^{13,14} and should be an analogue of dethio-tetra (methylthio) chetomin¹⁵. The planar structure of **1** was deduced

unambiguously from analysis of the 2D-NMR spectroscopic data, including ^1H – ^1H COSY, HSQC, and HMBC experiments (Fig. 1A and 1B). However, no NOESY correlations were observed that enabled relative configuration of **1**.

Although it is hard to determine configuration of tryptophan-derived epidithiodioxopiperazines for crystallization is difficult, **1** was recrystallized in CHCl_3 containing a small amount of MeOH, so the crystal of compound **1** was subjected to single-crystal X-ray diffraction analysis with Cu K α radiation, which unambiguously confirmed the structure. The result indicated a 3R, 5S, 10bR, 11aR, 3'S and 6'S absolute configuration (Fig. 1C) and **1** was named as Chaetocochins G.

Chaetocochins G (**1**), colorless needle crystals; mp 209.6°C ; $[\alpha]_D^{20} + 198$ ($c = 0.61$, CDCl_3); UV (CHCl_3) λ_{max} (log ϵ) 217 (4.79), 295 (4.06) nm; IR (KBr) ν_{max} 3399, 3327, 2919, 1667, 1647, 1632, 1605, 1421, 1385, 1058, 751 cm^{-1} ; CD (CDCl_3) 303 ($[\theta]$, +54169), 257 ($[\theta]$, +29483) nm; ^1H and ^{13}C NMR data, see Table 1; (+)-HRESIMS m/z 793.1934 $[M + Na]^+$ (calcd for $C_{35}H_{42}N_6NaO_6S_4^+$, 793.1941).

Compound **2** was isolated as a yellow amorphous powder. The sodiated molecular ion peak at m/z 354.0883 $[M + Na]^+$ (calcd 354.0883) observed in the HRESIMS corresponded to a molecular formula of $C_{16}H_{17}N_3O_3S$. The IR absorption bands at 1639, 1674 and 3429 cm^{-1} implied the presence of hydroxyl group and carbonyl groups. Comparison of ^1H NMR data (Table 2) indicated that **2** had the same scaffold as oidioperazine C¹⁶. The absence of the methoxyl signal at δ_H 3.15, together with the presence of an additional S-methyl (δ_H 2.08) and a N-methyl (δ_H 3.24), indicated the structure of **2** as shown (Fig. 1A). The cross-peaks of H-NCH₃ (δ_H 3.24) to C-1 (δ_C 161.7) and C-3 (δ_C 75.0) in the HMBC spectrum of **2** indicated that the N-methyl group was located at N-2. Similarly, the S-methyl group (δ_H 2.08) was located at C-3 (δ_C 75.0) (Fig. 1B).

The absolute configuration of **2** was determined by comparing its experimental and calculated ECD spectra. The cotton effects in the experimental ECD spectrum were consistent with those in calculated ECD curve of (3R)-**2** (Fig. 2). So, the structure of **2** was determined to be 3R configuration and named as Oidioperazines E.

Oidioperazines E (**2**): yellow amorphous powder; $[\alpha]_D^{20} - 190$ ($c = 2.07$, CDCl_3); UV (CHCl_3) λ_{max} (log ϵ) 227 (4.24), 339 (4.16) nm; IR (KBr) ν_{max} 3429, 2928, 1674, 1639, 1530, 1432, 1103, 740 cm^{-1} ; CD (CDCl_3) 236 ($[\theta]$, +35236), 335 ($[\theta]$, -79145) nm; ^1H NMR and ^{13}C NMR data, see Table 2; (+)-HRESIMS m/z 354.0883 $[M + Na]^+$ (calcd for $C_{16}H_{17}N_3NaO_3S^+$, 354.0883).

Compound **3** was isolated as colorless cubic crystals. The molecular formula of **3** was determined to be $C_{16}H_{19}N_3O_4S$ by HRFABMS (m/z 372.0988 $[M + Na]^+$, calcd. 372.0986). The IR spectrum of **3** gave the absorption of hydroxyl group (3325 cm^{-1}), and carbonyl groups (1685 and 1645 cm^{-1}).

The ^1H NMR data of **3** (Table 2) exhibited resonances for mono-substituted indole system at δ_H 7.70 d, 7.00 dd, 7.05 dd, 7.27, and 7.08 s, a S-methyl at δ_H 0.64, a N-methyl at δ_H 2.94, two methylene groups at δ_H 3.12/3.75 and 3.56/3.82. Analogous resonances consistent with the presence of these functionalities appeared in the ^{13}C NMR data of **3** (Table 2). According to the DEPT and HSQC spectra analysis of **3**, two sp^3 quaternary carbons bearing heteroatoms (δ_C 77.7, 84.1) and two carbonyl groups (δ_C 167.9, 170.3) could be observed.

The S-methyl moiety was located at the C-3 positions, as supported by the HMBC correlations (Fig. 1B) between H-SCH₃/C-3. N-methyl assigned at the C-2 positions from the HMBC correlations between H-NCH₃ from C-3 and C-1. Therefore, the planar structure of **3** is determined to be an analogue of Chetoseminudins B⁴.

As mentioned above, no NOESY correlations were observed to determine the relative configuration of **3**. The absolute configuration of **3** was determined by the X-ray single crystal diffraction analysis with Cu K α radiation. The results indicated that the crystal structure of compound **3** is shown in Figure 1C, and its absolute configuration was determined as 3R, 6S and named Chetoseminudin E.

Table 1 | NMR data [CDCl_3 , 400 MHz (^1H), 100 MHz (^{13}C)] for Chaetocochins G

position	δ_C	δ_H (J in Hz)
1	166.04 s	
2-NCH ₃	30.86 q	3.20 s
3	73.43 s	
3-SCH ₃	14.49 q	2.30 s
3-CH ₂ OH	64.41 t	3.84 m
		4.32 d (8.06)
4	164.24 s	
5	81.7 d	6.14 d (2.40)
6		5.22
6a	149.8 s	
7	110.4 d	6.73 d (6.87)
8	131.06 d	7.25 t (7.61)
9	119.8 d	6.87 td (7.49, 0.6)
10	124.61 d	7.27 d (8.12)
10a	127.9 s	
10b	72.97 s	
11	44.7 t	3.34 d (14.30)
		3.58 d (14.30)
11a	68.56 s	
11a-SCH ₃	15.89 q	2.00 s
1'	165.96 s	
2'-NCH ₃	29.43 q	2.78 s
3'	71.3 s	
3'-SCH ₃	13.58 q	2.10 s
3'-CH ₂ OH	63.98 t	3.09 d (11.85)
		3.74 dd (11.85, 6.58)
4'	166.62 s	
5'-NCH ₃	28.81 q	3.12 s
6'	73.15 s	
6'-SCH ₃	13.46 q	2.24 s
7'	32.8 t	3.18 d (15.17)
		3.88 d (15.17)
8'	107.6 s	
9'	125.5 d	7.01 s
10a'	134.8 s	
11'	111.9 d	7.04 d (7.69)
12'	122.74 d	6.94 t (7.92)
13'	120.15 d	7.03 t (7.57)
14'	119.79 d	7.57 d (7.73)
14a'	129.6 s	

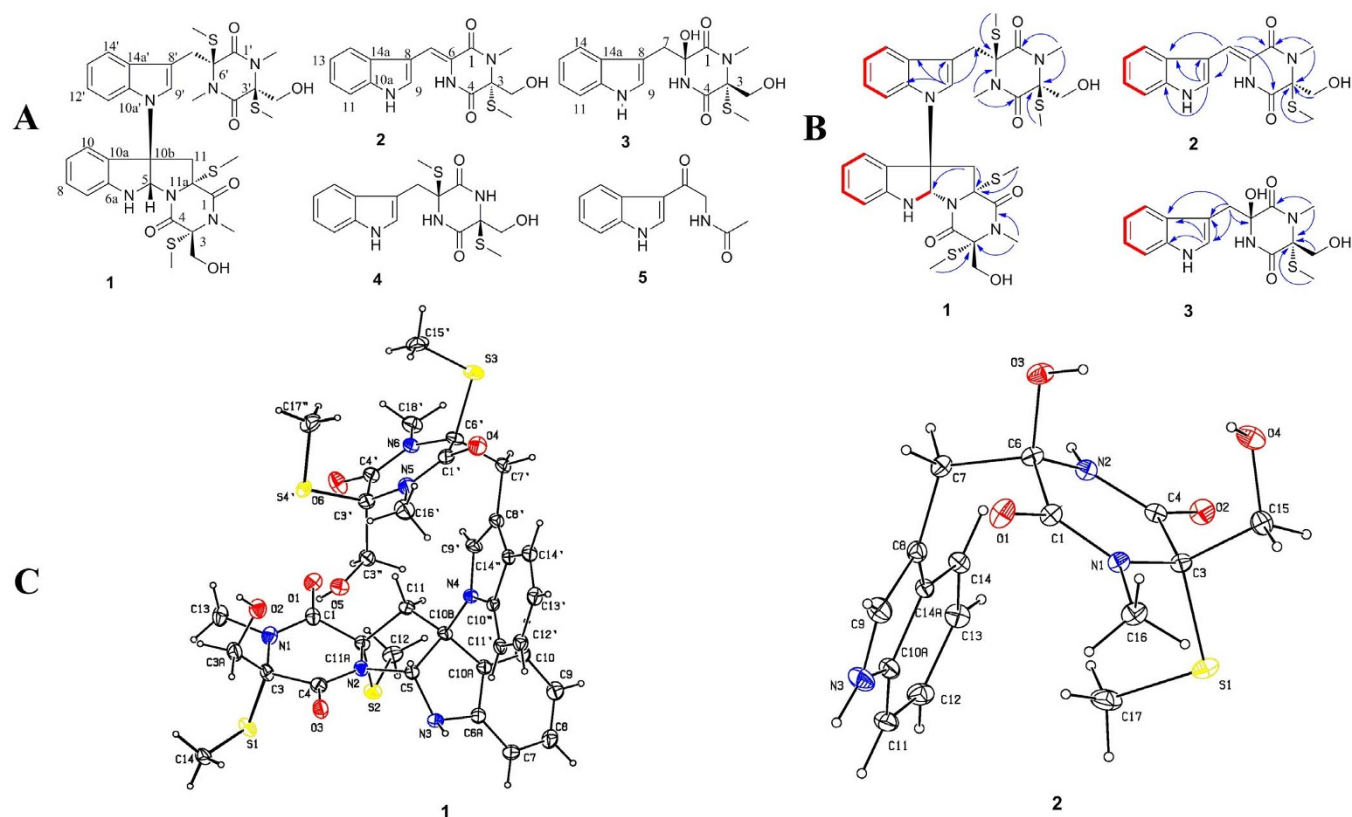


Figure 1 | Chemical structures of the isolated compounds. (A) Isolated compounds from extracts of fungus *Chaetomium sp* 88194 fermented rice substrate. (1–5). (B) Selected ^1H – ^1H COSY (red bold lines), and HMBC (H \rightarrow C) correlations. (C) ORTEP drawing of Chaetocochins G (1) and 3.

Chetoseminudin E (3): colorless cubic crystals; mp 193.3°C; $[\alpha]_{\text{D}}^{20} +54$ ($c = 0.64$, CH_3OH); UV (CHCl_3) λ_{max} (log ϵ) 219 (4.66), 281 (3.89) nm; IR (KBr) ν_{max} 3349, 3325, 2920, 1685, 1645, 1427, 1397, 1242, 1056, 752 cm^{-1} ; CD (CDCl_2) 267 ($[\theta]$, +24809), 299 ($[\theta]$, –4996) nm; ^1H NMR and ^{13}C NMR data, see Table 2; (+)-HRESIMS m/z 372.0988 $[\text{M} + \text{Na}]^+$ (calcd for $\text{C}_{16}\text{H}_{19}\text{N}_3\text{NaO}_3\text{S}_2^+$, 372.0986).

Chaetocochins G (1) causes proliferation inhibition and G2/M phase arrest in MCF-7 cells. All compounds were evaluated for cytotoxic effect against MCF-7 cells, together with one noncancerous human pulmonary epithelial cell line BEAS-2B, using MTT method¹⁷. 5-fluorouracil (5-Fu) was selected as positive control. As showed in Figure 3A, Chaetocochins G exhibited more potent cytotoxicity than 5-Fu (IC_{50} values was 16.9 $\mu\text{g/mL}$). The IC_{50} values of 48 h against

Table 2 | NMR data [CDCl_3 , 400 MHz (^1H), 100 MHz (^{13}C)] for Oidioperazines E (2) and Chetoseminudin E (3)

position	2 in CD_3OD		3 in CD_3OD	
	δ_{C}	δ_{H} (J in Hz)	δ_{C}	δ_{H} (J in Hz)
1	161.7 s		170.3 s	
3	75.0 s		77.7 s	
4	163.75 s		167.9 s	
6	120.66 s		84.1 s	
7	110.38 d	7.32 d (0.73)	36.9 t	3.13 d (14.0) 3.75 d (14.0)
8	108.37 s		109.3 s	
9	125.3 d	7.77 d (0.50)	126.4 d	7.08 s
10a	136.3 s		137.9 s	
11	111.38 d	7.43 d (8.04)	120.3 d	7.70 d (7.7)
12	122.38 d	7.21 dd (8.29, 6.93)	120.1 d	7.00 dd (8.1, 7.2)
13	120.09 d	7.14 dd (8.29, 7.04)	122.5 d	7.05 dd (8.1, 7.3)
14	118.01 d	7.68 d (7.84)	112.3 d	7.27 d (7.9)
14a	127.08 s		129.6 s	
2-NCH ₃	27.55 q	3.24 s	29.7 q	2.94 s
3-CH ₂ OH	62.57 t	3.87 d (11.67) 4.27 d (11.67)	64.6 t	3.82 d (11.4) 3.56 d (11.4)
3-SCH ₃	10.52 q	2.08 s	9.7 q	0.64 s

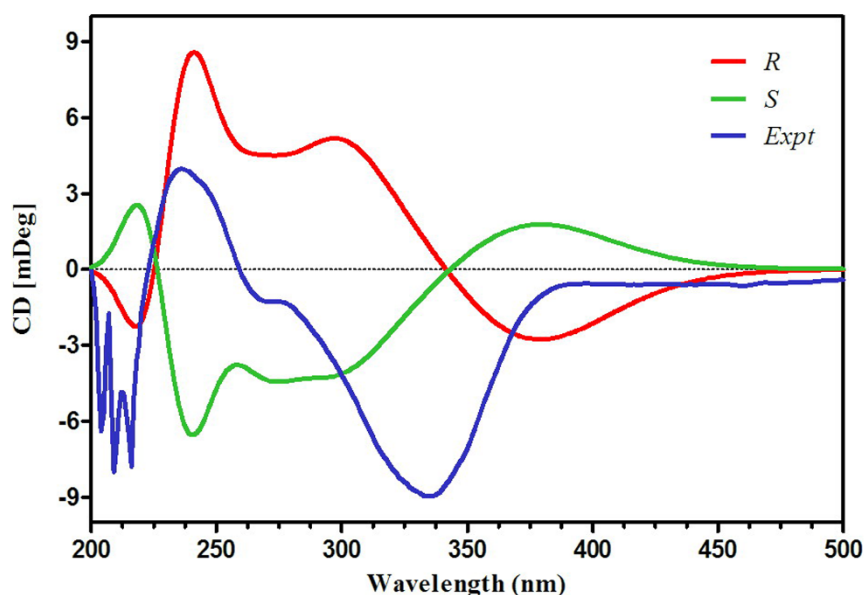


Figure 2 | Comparison of experimental and calculated ECD spectra of Oidiopiperazines E (2) and the stereoisomers (3S) and (3R).

MCF-7 and Beas-2B cell were 8.3, and 9.7 $\mu\text{g/mL}$. Compounds 2, 3, 4 and 5 did not show obvious cytotoxicity ($\text{IC}_{50} > 40 \mu\text{g/mL}$). So Chaetocochins G (1) was chosen for a further investigation.

Cell cycle is important for the proliferation of cancer¹⁸. To investigate cell cycle perturbations in MCF-7 cells induced by Chaetocochins G, flow cytometric analysis was performed after treatment at various concentrations (0, 5, 10, and 20 $\mu\text{g/mL}$) for 48 h. The results (Fig. 3B) revealed that Chaetocochins G arrested the cell cycle at the G2/M phase in MCF-7 cells in a concentration-dependent manner, which induced a corresponding increase percentage of cells in the G2/M-phase (7.83%, 19.17%, and 17.22%, compared to 2.8% in untreated cells) and decrease in the S-phase (37.71%, 26.79%, and 26.57%, compared to 42.76% in untreated cells).

Morphological changes of MCF-7 cells treated with Chaetocochins G. The morphological changes were examined using an invert light microscope as well as a fluorescence microscope after acridine orange (AO) and ethidium bromide (EB) double staining¹⁹. As shown in Figure 4A, cell shrinkage and abnormal morphological features could be observed in 5.0, and 10.0 $\mu\text{g/mL}$ Chaetocochins G treated groups. What's more, shrunk or colored orange cells that indicated apoptosis²⁰ were observed both on the coverslips and suspension during fluorescence microscope examination (Figure 4B, 4C). On the contrary, the untreated cells exhibited large green nuclei indicating the intact cell membranes.

Chaetocochins G (1) causes MCF-7 cell death by apoptosis. To determine whether Chaetocochins G mediated inhibition of growth and proliferation was associated with apoptosis, the flow cytometry apoptosis assay was performed using Annexin V and PI staining^{20–23}.

After treatment at various concentrations (0, 5, 10, and 20 $\mu\text{g/mL}$) for 48 h, the apoptosis of the cells were detected. As shown in Figure 5 the apoptotic cells accumulated in a dose-dependent manner from 26.24% to 92.99%. These results demonstrate that Chaetocochins G induced apoptosis of MCF-7 cells.

Chaetocochins G (1) changes the expression of apoptotic-related proteins. Among the caspase-family, caspase-3 is considered to be a critical effector and the activation of caspase-3 could result in PARP degradation²⁴. Bak and Bax have been categorized as prodeath members of Bcl-2 family. Protein, such as cytochrome c, could

release into cytoplasm from the mitochondria when the Bak and Bax homo-oligomerization on the mitochondrial membrane. Meanwhile, antiapoptotic Bcl-2 members could prevent mitochondrial protein release by interacting with and inhibiting both Bak and Bax²⁵.

MCF-7 cells were treated with Chaetocochins G as describe above. Changes of apoptosis-related protein, including Bax, Bcl-2, cleaved caspase-3 and PARP, were assessed by western blot analysis. β -actin was used as an internal control and relative optical density of proteins were compared with β -actin. As shown in Figure 6, the Bax protein levels increased dose dependently. In contrast, anti-apoptotic protein Bcl-2 declined upon Chaetocochins G treatment. Chaetocochins G-induced activation of caspase-3 was evidenced by appearance of cleaved caspase-3 and PARP (poly ADP-ribose polymerase)²⁶ in a concentration-dependent manner. All of the results above indicated that Chaetocochins G could induce apoptosis in MCF-7 cells.

In conclusion, the current study describes the isolation and identification of three new indole diketopiperazines (1–3) and two known compounds (4, 5) from the extracts of *Chaetomium sp* 88194. All the compounds were evaluated for the cytotoxicity against MCF-7 cell line. The results indicated that Chaetocochins G (1) displayed much more potent inhibitory activity than the common chemotherapeutic agent 5-fluorouracil, with IC_{50} values of 8.3 $\mu\text{g/mL}$, and induced cell cycle arrest at the G2/M phase in MCF-7 cells, accompanied by initiation of apoptosis. Further study demonstrated that Chaetocochins G induced cellular apoptosis via the activation of the Caspase 3, PARP, and Bax up-regulation as well as Bcl-2 inhibition. This paper is the first report for apoptosis-inducing effects of tryptophan-derived epidithiodioxopiperazines, and provides an insight into their anticancer mechanism. These results suggest that indole diketopiperazines from endophytic *Chaetomium sp* 88194 may be potential resource for anticancer drug research and discovery.

Methods

General experimental procedures. Melting points (uncorrected) were determined on a Beijing Tech X-5 microscopic melting point apparatus (Beijing Tech Instrument Col. Ltd, Beijing, China). Optical rotations were determined in CHCl_3 or MeOH on a Perkin-Elmer 341 polarimeter. UV and FT-IR spectra were determined using PerkinElmer Lambda 35 and Bruker Vertex 70 instrument, respectively. HRESIMS was performed on a Thermo Scientific LTQ-XL mass spectrometer. NMR spectra were recorded on a Bruker AM-400 NMR spectrometer and chemical shifts were referenced to the solvent peaks for CD_3OD (δ_{H} 3.31/ δ_{C} 49.0) or CDCl_3 (δ_{H} 7.26/ δ_{C} 77.16). The CD spectra were obtained on a JASCO J-810 spectrometer. X-ray crystallographic data were collected from Bruker Smart APEX-II CCD diffractometer

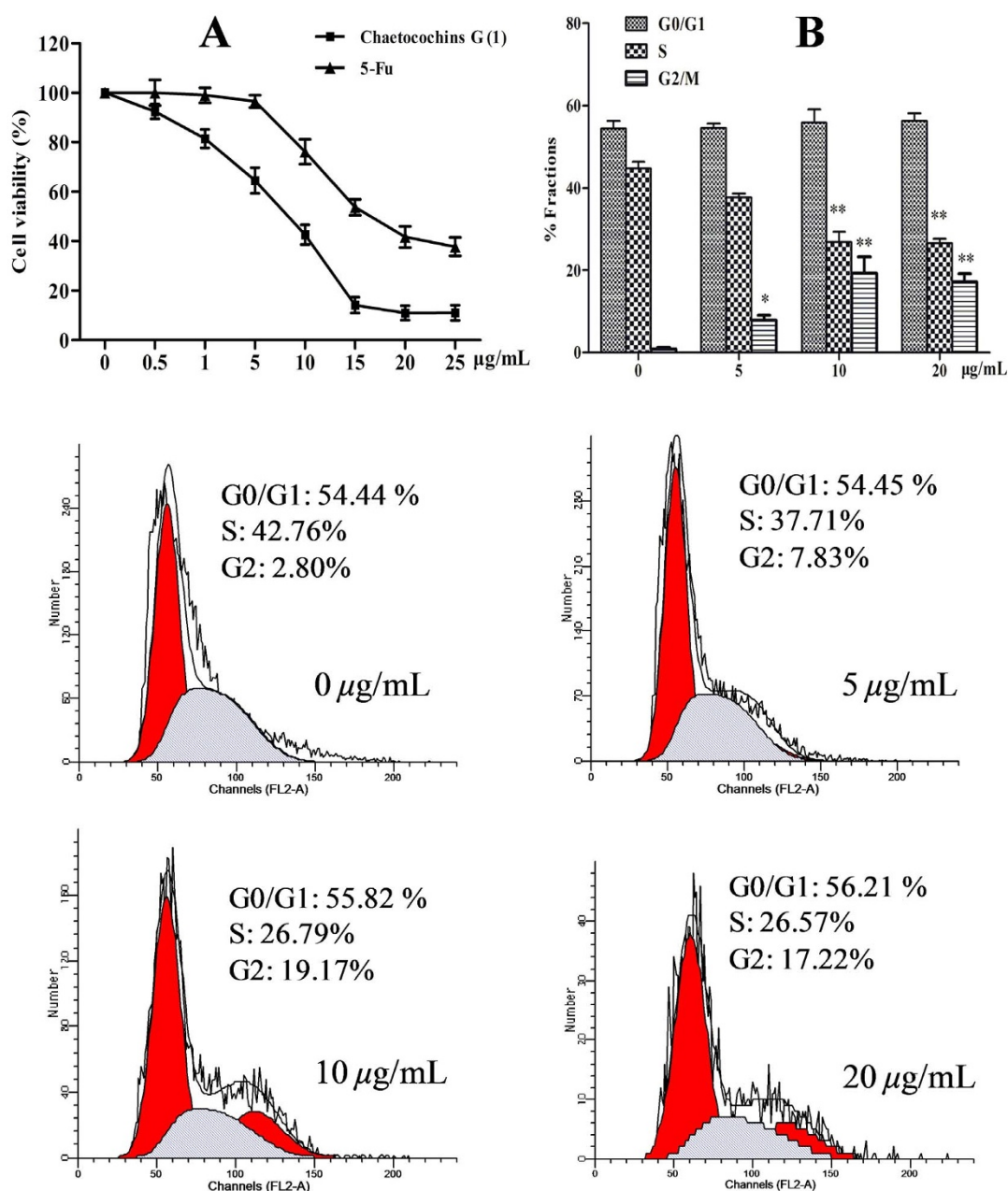


Figure 3 | Chaetocochins G (1) causes inhibitory proliferation and G2/M phase arrest in MCF-7 cells. (A) Chaetocochins G inhibits the proliferation of MCF-7 cells. Cells were treated with various concentrations of Chaetocochins G for 48 h. Cell viability was detected using MTT assay, 5-Fu was used as positive control. (B) Cell cycle progression of Chaetocochins G in MCF-7 Cells. Data are presented as the means \pm SD of three experiments, * $P < 0.05$, ** $P < 0.01$ compared to the control group.

equipped with graphite-monochromatized Cu K α radiation ($\lambda = 1.54178 \text{ \AA}$). HPLC isolation was performed on waters 2535 pump and a waters 2998 detector using a C_{18} column (5 μm , $10 \times 250 \text{ mm}$, SunFireTM Prep C_{18}) and $\text{MeOH-H}_2\text{O}$ or $\text{CH}_3\text{CN-H}_2\text{O}$ as the mobile phase at 2.0 mL/min flow rate. MPLC was carried out with a QuikSep-50 chromatography system (H&E Co., Ltd, Beijing, China). TLC was carried out using glass-precoated silica gel GF254 (Qingdao Marine Chemical, Inc., Qingdao, China) and visualized under UV light. Silica gel (100–200 mesh and 200–300 mesh, Qingdao Marine Chemical Inc., Qingdao, China), ODS (50 μm , YMC, Kyoto, Japan), and Sephadex LH-20 (Pharmacia Biotech AB, Uppsala, Sweden) were used for column chromatography.

Fungal strain and identification. The strain of the fungus obtained from China Forestry Culture Collection Center (CFCC, Beijing, China) was isolated from the *Cymbidium goeringii*, which was collected from Xinning, Hunan Province of China, in November 2008. The strain was purified and identified belonging to the *Chaetomium* sp by molecular identification. The DNA sequence data from the fungus were deposited at GenBank with accession number KP171518, and the strain was deposited at Hubei Key Laboratory of Natural Medicinal Chemistry and Resource

Evaluation, School of Pharmacy, Tongji Medical College, Huazhong University of Science and Technology, Wuhan, PR China.

Fermentation and isolation. The fermentation was carried out in 40 fernbach flasks (1000 mL), each containing 200 g of rice and distilled H_2O (200 mL). After autoclaving at 121°C , 15 psi for 30 min, each flask cooling to room temperature was inoculated with the fresh mycelium and incubated at 25°C for 28 days.

The fermented solid rice medium (8.0 kg) was soaked with 95% aqueous EtOH (40 L \times 3, 1 day for each time) at room temperature. The solvent was evaporated in vacuo to afford a residue (22.0 g), which was then partitioned between ethyl acetate (3 L \times 3) and aqueous (3 L). On evaporation, the organic phase (250 g) was subjected to silica gel (200–300 mesh) column chromatography and eluted with a MeOH-CHCl_3 gradient to give four fractions, A–D. Fractions C (2.7 g) was chromatographed over ODS by MPLC and eluted with a $\text{MeOH-H}_2\text{O}$ gradient to yield four fractions (C_A-C_D).

Subfraction C_A was further separated by semipreparative HPLC ($\text{CH}_3\text{CN-H}_2\text{O}$, 60:40, flow rate: 2 mL/min) to yield compounds 1 (67.31 mg, t_R 20.3 min). Subfraction C_B was further separated over Sephadex LH-20 eluting with CHCl_3 –

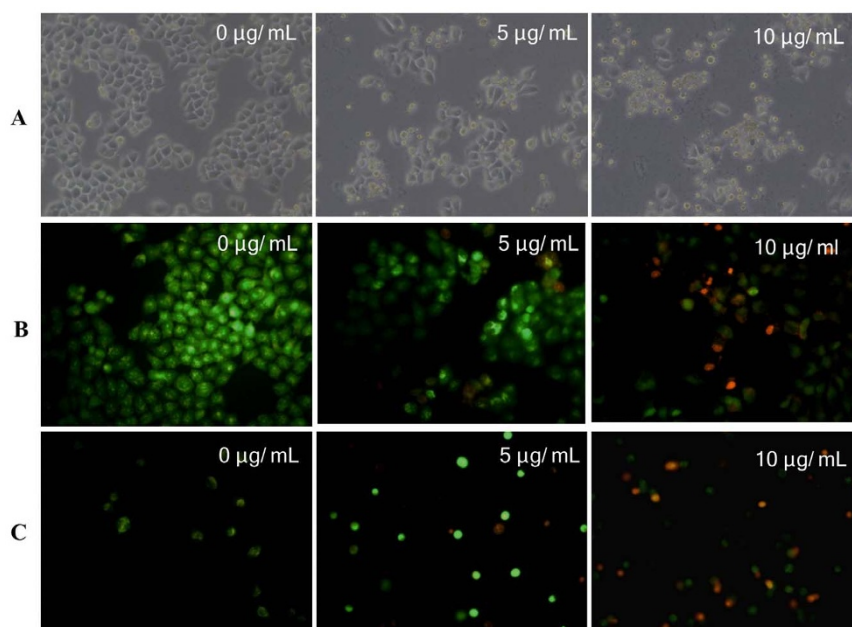


Figure 4 | Morphological changes of MCF-7 cells induced by Chaetocochins G. (A) Cells shrinkage and abnormal morphological features could be observed (100 \times). (B) Cells on coverslips treated with Chaetocochins G at 5.0 and 10 $\mu\text{g/mL}$, stained with AO/EB (100 \times). (C) Cells in suspension treated with Chaetocochins G at 5.0 and 10 $\mu\text{g/mL}$, stained with AO/EB (100 \times).

MeOH (1 : 1) to give three subfractions (C_{BA} – C_{BC}). Subfraction C_{BB} was further purified by semi-preparative HPLC eluted with MeOH–H₂O (40 : 60, flow rate: 2 mL/min) to give compounds 3 (8.5 mg, t_R 28.9 min), compounds 2 (10.37 mg, t_R 28 min) was obtained from C_{BC} through semi-preparative HPLC eluted with CH₃CN–H₂O (65 : 35, flow rate: 2 mL/min). Subfraction C_C was purified by Sephadex LH-20 column chromatography eluting with CHCl₃–MeOH (1 : 1) to give two subfractions (C_{CA} – C_{CB}). Then, C_{CB} was chromatographed over ODS by MPLC and eluted with a MeOH–H₂O gradient to yield compounds 4 (1.95 mg) and 5 (5.8 mg).

Crystallographic Data and X-ray Structure Analysis. Colorless needle crystals of Chaetocochins G (1) were obtained from CHCl₃ containing a small amount of MeOH at room temperature. Crystal data were obtained on a Bruker Smart APEX-II CCD single-crystal X-ray diffractometer with the Cu K α (λ = 1.54178 Å). Structure solution and refinement were performed with the SHELXL-97. Crystal data of 1: $C_{35}H_{42}N_6O_6S_4 \cdot H_2O$ (M = 789.00); needle crystal (0.20 \times 0.20 \times 0.10 mm); space group $P2_1$; unit cell dimensions a = 13.3191(3) Å, b = 13.7927(3) Å, c = 21.8874(5) Å, α = 90.00°, β = 96.0450(10)°, γ = 90.00°, V = 3998.50(15) Å³; Z = 4; T = 296(2) K; ρ_{calcd} = 1.311 Mg/m³; absorption coefficient 2.623 mm^{−1}, $F(000)$ = 1664, A total of 10529 reflections were collected in the range $2.03^\circ < \theta < 58.42^\circ$ with 10529 independent reflections [$R(\text{int})$ = 0.0000]; completeness to θ_{max} was 97.3%; full-matrix least-squares refinement on F^2 ; the number of data/parameters/restraints were 10529/1029/47; goodness-of-fit on F^2 = 1.067; final R indices [$I > 2\sigma(I)$] R_1 = 0.0437, wR_2 = 0.1226; R indices (all data) R_1 = 0.0578, wR_2 = 0.1312; absolute structure parameter 0.015(12).

Colorless cubic crystals of Chetoseminudin E (3) were obtained from CH₃OH at room temperature. Crystal data were obtained on a Bruker Smart APEX-II CCD single-crystal X-ray diffractometer with the Cu K α (λ = 1.54178 Å). Structure solution and refinement were performed with the SHELXL-97. Crystal data of 3: $2(C_{16}H_{20}N_3O_4S) \cdot H_2O$ (M = 716.82); monoclinic crystal (0.71 \times 0.53 \times 0.40 mm); space group $P2_1$; unit cell dimensions a = 8.8404(2) Å, b = 14.4203(3) Å, c = 13.5625(2) Å, α = 90.00°, β = 92.8240(10)°, γ = 90.00°, V = 1726.86(6) Å³; Z = 2; T = 298(2) K; ρ_{calcd} = 1.379 Mg/m³; absorption coefficient 1.925 mm^{−1}, $F(000)$ = 756, A total of 21876 reflections were collected in the range $3.26^\circ < \theta < 68.72^\circ$ with 6000 independent reflections [$R(\text{int})$ = 0.0328]; completeness to θ_{max} was 96.9%; full-matrix least-squares refinement on F^2 ; the number of data/parameters/restraints were 6000/452/1; goodness-of-fit on F^2 = 1.042; final R indices [$I > 2\sigma(I)$] R_1 = 0.0284, wR_2 = 0.0785; R indices (all data) R_1 = 0.0286, wR_2 = 0.0787; absolute structure parameter 0.025(10).

Crystallographic data for the structures of Chaetocochins G (1) and Chetoseminudin E (3) have been deposited in the Cambridge Crystallographic Data Centre [deposition numbers: CCDC 1029222 (1), and CCDC 1029221 (3)]. Copies of these data can be obtained free of charge at www.ccdc.cam.ac.uk/conts/retrieving.html, email: (or from the Cambridge Crystallographic Data Centre, 12 Union Road, Cambridge CB21EZ, UK; fax: (+44) 1223-336-033; or e-mail: deposit@ccdc.cam.ac.uk).

Computational methods for ECD spectra. The conformational spaces for the 3R and 3S isomers of Odioperazines E (2) were explored using both BALLOON²⁷ and

confab²⁸ programs. The BALLOON program searches conformational space with genetic algorithm, whereas the confab program systematically generates diverse low energy conformations that are supposed to be close to crystal structures. Duplicate conformations were identified and removed when the root-mean-square (RMS) distance was less than 0.5 Å. The semi-empirical PM3 quantum mechanical geometry optimizations were performed on the conformations by using Gaussian 09 program. The remaining conformations were further optimized at B3LYP/6-31G* level of theory in dichloromethane solvent with IEFPCM3²⁹ solvation model by using Gaussian 09 program, and the duplicated conformations emerging after this calculations were removed according to the same RMS criteria above. The harmonic vibrational frequencies were performed to confirm the stability of the finally obtained conformers. The oscillator strengths and rotational strengths of 20 weakest electronic excitations of each conformer were calculated using the TDDFT methodology at the B3LYP/6-311++G** level of theory with dichloromethane as solvent by the IEFPCM solvation model implemented in Gaussian 09 program. The ECD spectra for each conformer were then simulated by using a Gaussian function with a bandwidth σ of 0.45 eV. The calculated spectra for each conformation were combined after Boltzmann weighting according to their population contribution.

Cell culture and cell viability assay. MCF-7 human breast cancer cells, purchased from the cell bank of the Basic Medical College of Huazhong University of Science and Technology, were cultured in DMEM medium (Solarbio, Peking, People's Republic of China), supplemented with 10% fetal bovine serum (Sijiqing, Hangzhou, People's Republic of China), 100 U/mL penicillin, and 100 $\mu\text{g/mL}$ streptomycin. Cultures were maintained in an incubator (Thermo Fisher Scientific, Marietta, USA) with 5% CO₂ at 37°C.

The viability of cells was performed using an MTT [3-(4,5-dimethylthiazol-2-yl)-2,5-diphenyltetrazolium bromide] (Biosharp, Hefei, People's Republic of China) method in 96-well microplates, as reported previously³⁰, with slight modification. Cells were plated in 96-well culture plates (9 \times 10³ per well) and allowed to adhere for 12 h before treated with Chaetocochins G at a series of concentration (0, 0.5, 1, 5, 10, and 20 $\mu\text{g/mL}$) for 48 hours. Add 20 μL MTT (5 mg/mL) per well was added prior to 4 h incubation at 37°C. Upon medium removal, formazans depositing on the plate were dissolved in 150 μL DMSO, then, the cell viability was detected by a Thermo Multiskan MK3 microplate reader (Thermo Scientific, Helsinki, Finland) at λ = 492 nm, and the IC₅₀ values were obtained from the MTT viability curves using GraphPad Prism 4.0.

Cell morphology. After incubation with various concentrations of Chaetocochins G (0, 5, and 10 $\mu\text{g/mL}$) for 48 h, a staining method using AO (Solarbio, Peking, People's Republic of China) and EB (Solarbio, Peking, People's Republic of China) was performed and photographed using a fluorescence microscope (Olympus BX-51, Tokyo, Japan).

Cell cycle analysis. The cell cycle analysis was detected with a cell cycle and apoptosis analysis kit (Beyotime, Haimen, People's Republic of China). MCF-7 cells were exposed to Chaetocochins G (0, 5, 10 and 20 $\mu\text{g/mL}$) and incubated for 48 h. Then, the cells were harvested and washed with ice-cold PBS buffer, fixed with 70% alcohol

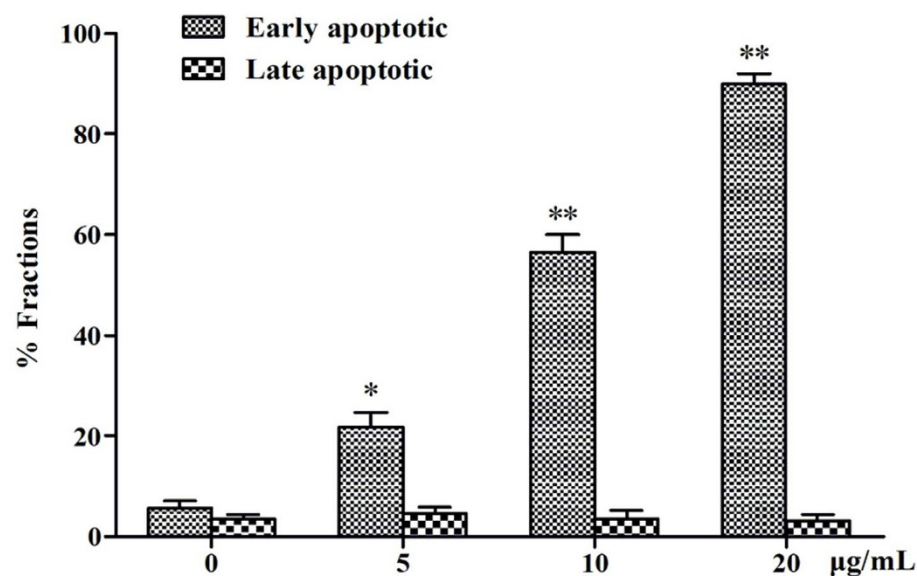
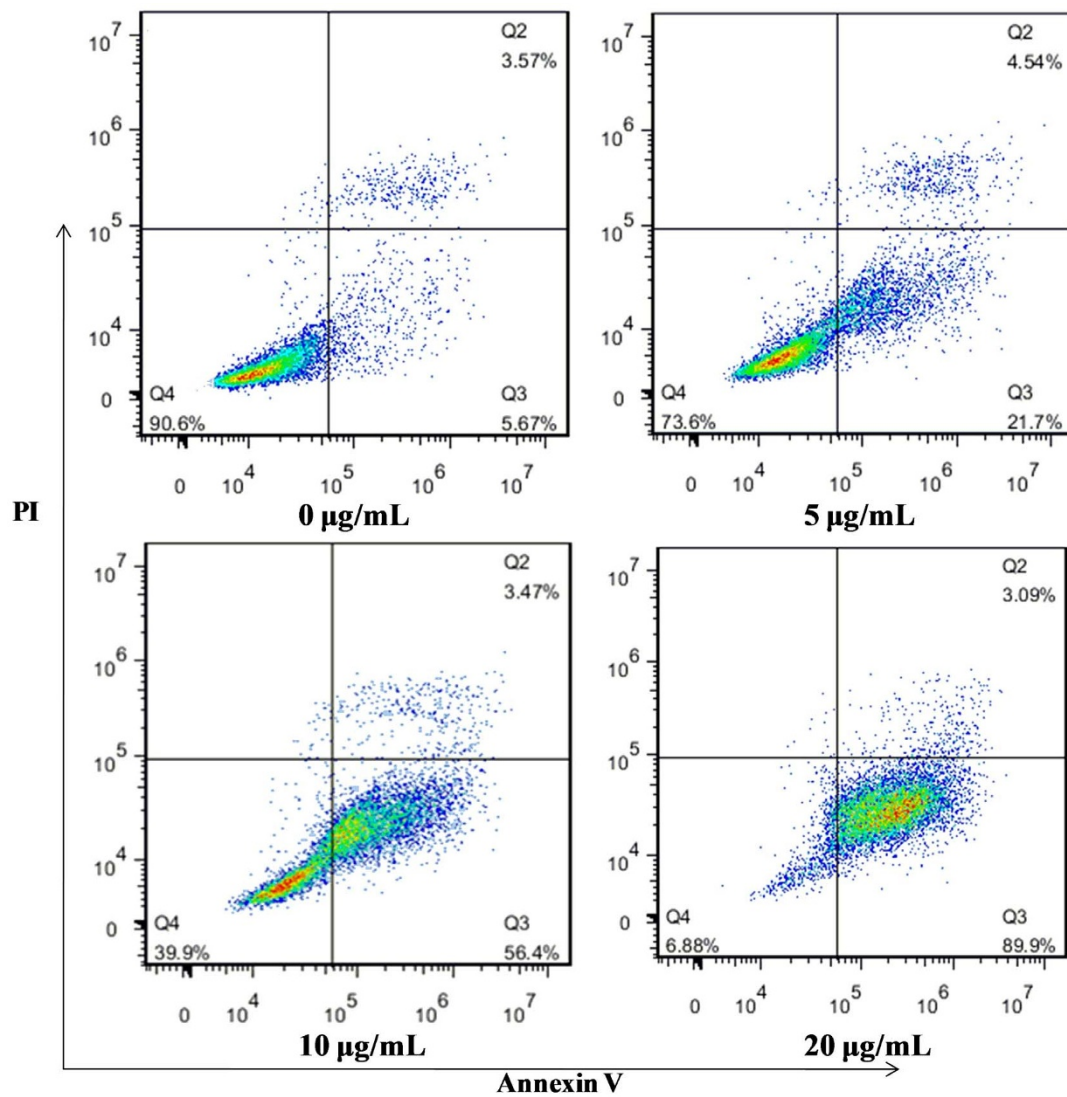


Figure 5 | Analysis of apoptosis in Chaetochins G treated MCF-7 Cells. Cells were treated with Chaetochins G at various concentrations (0, 5, 10, and 20 $\mu\text{g/mL}$) for 48 h, then collected and stained with annexin V/PI, and subjected to flow cytometry. Data are presented as the means \pm SD of three experiments. * $P < 0.05$, ** $P < 0.01$ compared to the control group.

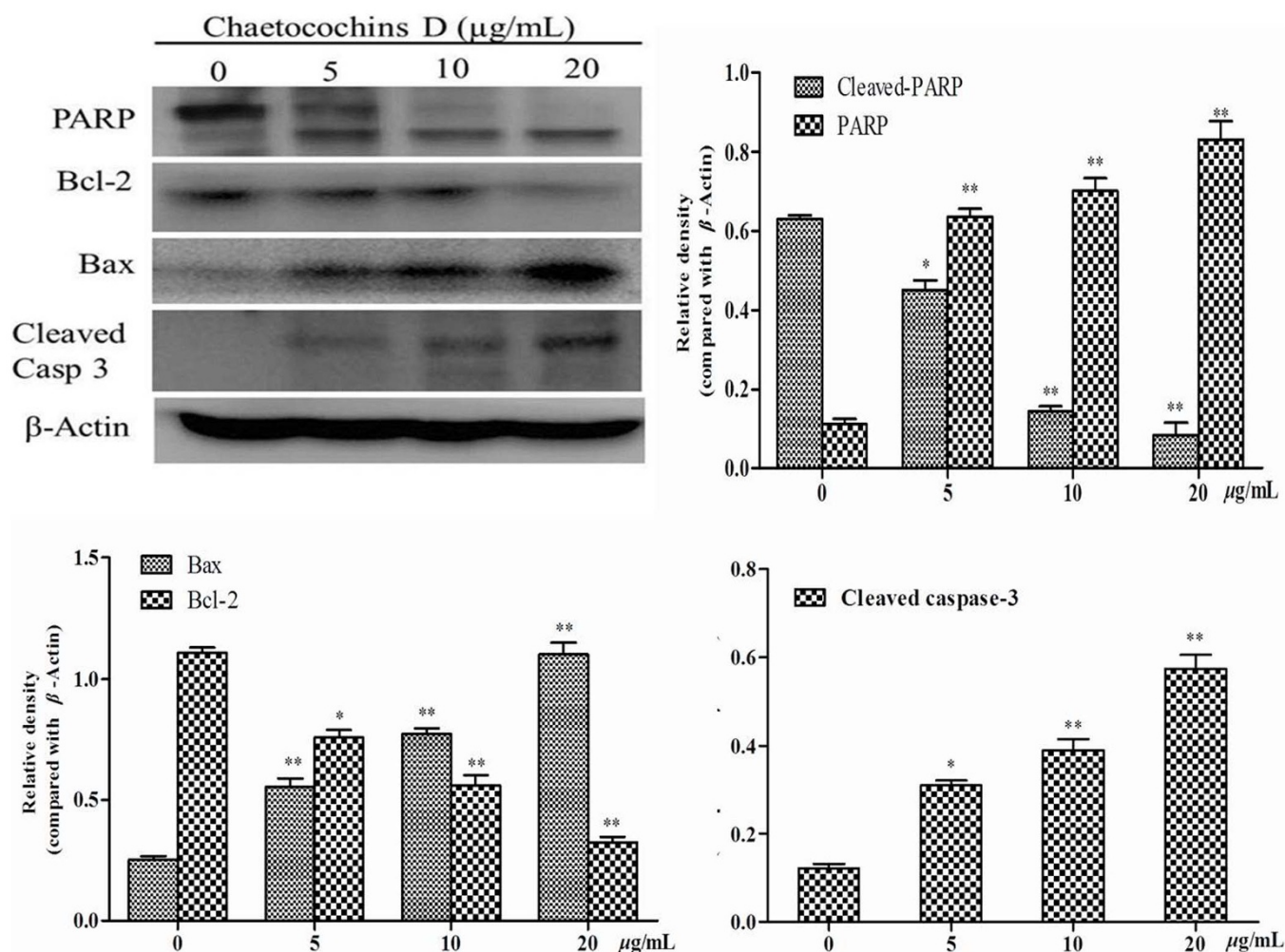


Figure 6 | Changes of apoptosis-related protein in MCF-7 cells after Chaetocochins G treated. The relative density was detected by Image J, data are presented as the means \pm SD of three experiments, significant differences from the control value (0 μ g/mL) are indicated by * $p < 0.05$, ** $p < 0.01$.

at 4°C for 12 h, and stained with propidium iodide (PI) in the presence of 1% RNAase A. After 15 min incubation at 37°C, the cells were analyzed by a flow cytometry (Becton Dickinson, San Jose, USA). The gated data were analyzed by modfit softwares (Verity Software House, Topsham, Maine, USA).

Flow cytometric and western blotting analysis of cell apoptosis. Apoptosis assay was performed using an apoptosis detection kit (Keygen, Nanjing, People's Republic of China) according to the manufacturer's instructions. Briefly, after exposure to Chaetocochins G (0, 5, 10 and 20 μ g/mL) for 48 h, cells were collected, washed with annexin-binding buffer, incubated with annexinV-FITC/PI for 15 min and analyzed by a flow cytometry (Becton Dickinson, San Jose, CA, USA).

Western blotting. Western blotting analysis was performed as described³¹. MCF-7 cells were treated with Chaetocochins G in 0, 5, 10 and 20 μ g/mL. After 48 h, cells were harvested and washed with ice-cold PBS and then lysed in ice cold RIPA lysis buffer for 30 min. The lysate was centrifuged at 12000 rpm for 15 min at 4°C and the supernatant was collected, the total protein concentration was determined using the BCA assay; the proteins were then dissolved in SDS sample buffer and denatured. Proteins were separated using 10% SDS-PAGE, and then transferred to PVDF (polyvinylidene fluoride) (Bio-Rad, Hercules, CA) membranes. After incubated overnight at 4°C with the respective primary antibodies, the horseradish peroxidase-conjugated secondary antibodies were added. Finally, the reactive band was identified using an enhanced chemiluminescent substrate to horseradish peroxidase.

Statistical analysis. Statistical analysis of the data was processed with GraphPad Prism 4.0 software. Statistical analysis of the data was expressed as mean \pm SD. Values were analyzed by one-way analysis of variance (ANOVA) using SPSS version 12.0 software. $p < 0.05$ were considered statistically significant.

- Zhang, H. W., Song, Y. C. & Tan, R. X. Biology and chemistry of endophytes. *Nat. Prod. Rep.* **23**, 753–771 (2006).

- Ge, H. M. *et al.* Chaetoglobins A and B, two unusual alkaloids from endophytic *Chaetomium globosum* culture. *Chem Commun.* 5978–5980 (2008), (DOI: 10.1039/b812144c).
- Li, G. Y., Li, B. G., Yang, T., Yan, J. F., Liu, G. Y. & Zhang, G. L. Chaetocochins A-C, epipolythiodioxopiperazines from *chaetomium cochliodes*. *J. Nat. Prod.* **69**, 1374–1376 (2006).
- Shashova, E. E. *et al.* Proteasome functioning in breast cancer: connection with clinical-pathological factors. *PLoS One* **9**, e109933 (2014).
- Porter, P. L. Global trends in breast cancer incidence and mortality. *Salud Publica Mex* **51**, s141–s146 (2009).
- Fujimoto, H., Sumino, M., Okuyama, E. & Ishibashi, M. Immunomodulatory constituents from an ascomycete, *chaetomium seminudum*. *J. Nat. Prod.* **67**, 98–102 (2004).
- Martínez-Luis, S., Gómez, J. F., Spadafora, C., Guzmán, H. M. & Gutiérrez, M. Antitrypanosomal alkaloids from the marine bacterium. *Bacillus pumilus*. *Molecules* **17**, 11146–11155 (2012).
- Murray, A. W. Recycling the cell cycle: cyclins revisited. *Cell* **116**, 221–234 (2004).
- Buolamwini, J. K. Cell cycle molecular targets innovel anticancer drug discovery. *Curr Pharm Des.* **6**, 379–392 (2000).
- Taraphdar, A. K., Roy, M. & Bhattacharya, R. K. Natural products as inducers of apoptosis: Implication for cancer therapy and prevention. *Curr. Sci.* **80**, 1387–1396 (2001).
- Singh, B. N., Shankar, S. & Srivastava, R. K. Green tea catechin, epigallocatechin-3-gallate (EGCG): mechanisms, perspectives and clinical applications. *Biochem Pharmacol.* **82**, 1807–1821 (2011).
- Shankar, S., Ganapathy, S., Hingorani, S. R. & Srivastava, R. K. EGCG inhibits growth, invasion, angiogenesis and metastasis of pancreatic cancer. *Front Biosci.* **13**, 440–452 (2008).
- Saito, T., Suzuki, Y., Koyama, K., Natori, S., Iitaka, Y. & Kinoshita, T. Chetracin A and chaetocins B and C, three new epipolythiodioxopiperazines from *Chaetomium spp.* *Chem Pharm Bull.* **36**, 1942–1956 (1988).



14. Son, B. W., Jensen, P. R., Kauffman, C. A. & Fenical, W. New cytotoxic epidithiodioxopiperazines related to verticillin A from a marine isolate of the fungus *Penicillium*. *Nat Prod Lett* **13**, 213–222 (1999).
15. Kikuchi, T. *et al.* Dethio-tetra (methylthio) chemtomin, a new antimicrobial metabolite of *Chaetomium globosum* kinze ex fr. structure and partial synthesis from chetomin. *Chem. Pharm. Bull.* **30**, 3846–3848 (1982).
16. Li, L., Li, D., Luan, Y., Gu, Q. & Zhu, T. Cytotoxic metabolites from the antarctic psychrophilic fungus *Oidiodendron truncatum*. *J Nat Prod.* **75**, 920–927 (2012).
17. Alley, M. C. *et al.* Feasibility of drug screening with panels of human tumor cell lines using a microculture tetrazolium assay. *Cancer Res.* **48**, 589–601 (1998).
18. Evan, G. I. & Vousden, K. H. Proliferation, cell cycle and apoptosis in cancer. *Nature* **411**, 342–348 (2001).
19. Leite, M., Quinta-Costa, M., Leite, P. S. & Guimarães, J. E. Critical evaluation of techniques to detect and measure cell death – study in a model of UV radiation of the leukaemic cell line HL60. *Anal. Cell. Pathol.* **19**, 139–151 (1999).
20. Yu, H. Y., Zhang, X. Q., Li, X., Zeng, F. B. & Ruan, H. L. 2-Methoxyjuglone induces apoptosis in HepG2 human hepatocellular carcinoma cells and exhibits in vivo antitumor activity in a H22 mouse hepatocellular carcinoma model. *J Nat Prod.* **76**, 889–895 (2013).
21. Vermes, I., Haanen, C., Steffens-Nakken, H. & Reutelingsperger, C. A novel assay for apoptosis. Flow cytometric detection of phosphatidylserine expression on early apoptotic cells using fluorescein labelled Annexin V. *J Immunol Methods.* **184**, 39–51 (1995).
22. Verhoven, B., Schlegel, R. A. & Williamson, P. Mechanisms of phosphatidylserine exposure, a phagocyte recognition signal, on apoptotic T lymphocytes. *J Exp Med.* **182**, 1597–1601 (1995).
23. Nicoletti, I., Migliorati, G., Pagliacci, M. C., Grignani, F. & Riccardi, C. A rapid and simple method for measuring thymocyte apoptosis by propidium iodide staining and flow cytometry. *J Immunol Methods.* **139**, 271–279 (1991).
24. Ghavami, S. *et al.* Apoptosis and cancer: mutations within caspase genes. *J Med Genet.* **46**, 497–510 (2009).
25. Jiang, X. & Wang, X. Cytochrome C-mediated apoptosis. *Annu Rev Biochem.* **73**, 87–106 (2004).
26. Gobeil, S., Boucher, C. C., Nadeau, D. & Poirier, G. G. Characterization of the necrotic cleavage of poly(ADP-ribose) polymerase (PARP-1): implication of lysosomal proteases. *Cell Death Differ.* **8**, 588–594 (2001).
27. Vainio, M. J. & Johnson, M. S. Generating conformer ensembles using a multiobjective genetic algorithm. *J Chem Inf Model.* **47**, 2462–2474 (2007).
28. O'Boyle, N. M., Vandermeersch, T., Flynn, C. J., Maguire, A. R. & Hutchison, G. R. Confab-Systematic generation of diverse low-energy conformers. *J Cheminform.* **16**, 1–9 (2011).
29. Tomasi, J., Mennucci, B. & Cammi, R. Quantum mechanical continuum solvation models. *Chem Rev.* **105**, 2999–3093 (2005).
30. Luo, Z. *et al.* Cytotoxic alkaloids from the whole plants of *Zephyranthes candida*. *J Nat Prod.* **75**, 2113–2120 (2012).
31. Tong, Q. Y., He, Y., Zhao, Q. B., Qing, Y., Huang, W. & Wu, X. H. Cytotoxicity and apoptosis-inducing effect of steroidal saponins from *Dioscorea zingiberensis* wright against cancer cells. *Steroids.* **77**, 1219–1227 (2012).

Acknowledgments

We acknowledge Dr. X.-N. Li (Kunming Institute of Botany, Chinese Academy of Sciences) for the single crystal X-ray diffraction analyses.

Author contributions

Y.H.Z., G.Z. and Y.B.X. designed experiments. J.J.L. complete the computation section. W.M. and J.W.Z. wrote the paper. Q.Y.T. and H.R.M. conducted experiments. F.Q.W. isolated and identified of the compounds. H.P.S. analyzed data. J.P.W., H.F.X. and S.H. prepared the article in the journal's format. All authors reviewed the manuscript.

Additional information

Supplementary information accompanies this paper at <http://www.nature.com/scientificreports>

Competing financial interests: The authors declare no competing financial interests.

How to cite this article: Wang, F.-q. *et al.* Indole diketopiperazines from endophytic *Chaetomium* sp 88194 induce breast cancer cell apoptotic death. *Sci. Rep.* **5**, 9294; DOI:10.1038/srep09294 (2015).



This work is licensed under a Creative Commons Attribution 4.0 International License. The images or other third party material in this article are included in the article's Creative Commons license, unless indicated otherwise in the credit line; if the material is not included under the Creative Commons license, users will need to obtain permission from the license holder in order to reproduce the material. To view a copy of this license, visit <http://creativecommons.org/licenses/by/4.0/>